Chinese Chemical Letters 37 (2026) 111751

Contents lists available at ScienceDirect

Chinese Chemical Letters

journal homepage: www.elsevier.com/locate/cclet

Discovery of DHODH PROTAC degraders with anti-SARS-CoV-2 and influenza virus activity

Hongliang Wang[a,b,1], Yuanguo Li[c,1], Linjie Yan[a], Liyuan Ge[d], Wenhao Wang[c], Lei Zhao[a,*], Yuwei Gao[c,*], Wu Zhong[a,*]

[a] National Engineering Research Center for the Emergency Drug, Beijing 100850, China
[b] Army Medical University, NCO School, Shijiazhuang 050000, China
[c] Changchun Veterinary Research Institute, Chinese Academy of Agricultural Sciences, State Key Laboratory of Pathogen and Biosecurity, Key Laboratory of Jilin Province for Zoonosis Prevention and Control, Changchun 130122, China
[d] Song Li's Academician Workstation of Hainan University (School of Pharmaceutical Sciences), Yazhou Bay, Sanya 572024, China

ARTICLE INFO

Article history:
Received 28 June 2025
Revised 22 August 2025
Accepted 24 August 2025
Available online 25 August 2025

Keywords:
DHODH
PROTAC
SARS-CoV-2
Influenza virus
Coinfection

ABSTRACT

Coinfection with severe acute respiratory syndrome coronavirus 2 (SARS-CoV-2) and influenza virus exacerbates pulmonary inflammation and tissue damage, significantly increasing the risks of respiratory failure, acute respiratory distress syndrome (ARDS), and secondary bacterial infections. Currently, there are no approved therapeutic agents specifically targeting these two viruses' coinfection. Human dihydroorotate dehydrogenase (DHODH), a key enzyme catalyzing the fourth step in the *de novo* pyrimidine biosynthesis pathway through the oxidation of dihydroorotate to orotate, serves as the rate-limiting enzyme in pyrimidine biosynthesis. This critical metabolic checkpoint has emerged as a promising broad-spectrum antiviral target. In this study, we designed and synthesized a series of DHODH-targeting proteolysis-targeting chimeras (PROTACs), among which PROTACs **17** and **19** connected *via* flexible alkyl linkers were identified as the most potent molecules. Mechanistic investigations revealed that **17** and **19** induced DHODH degradation through the proteasome- and cereblon (CRBN)-dependent pathways. Remarkably, **17** and **19** exhibited significant antiviral activities against both influenza virus and SARS-CoV-2 *in vitro*. These findings collectively present a novel and effective strategy for the treatment of coinfection caused by SARS-CoV-2 and influenza virus.

© 2026 Published by Elsevier B.V. on behalf of Chinese Chemical Society and Institute of Materia Medica, Chinese Academy of Medical Sciences.

"Flucovid" refers to a disease caused by the coinfection with influenza virus and severe acute respiratory syndrome coronavirus 2 (SARS-CoV-2), presenting with both influenza and corona virus disease 2019 (COVID-19) symptoms including fever, cough, fatigue, headache, dyspnea, and loss of taste or smell, but excluding common cold symptoms such as sneezing, rhinorrhea/nasal congestion, and sore throat [1]. A recent meta-analysis employing a random-effects model within 95 % confidence intervals revealed that the prevalence of influenza coinfection among COVID-19 patients was 14 % (95 % confidence interval (CI): 8 %–20 %) [2]. Notably, pediatric and geriatric populations demonstrate higher incidence rates of coinfection [3]. Both SARS-CoV-2 and influenza viruses can directly attack pulmonary tissues, potentially inducing viral pneumonia. Coinfection may exacerbate pulmonary inflammation and injury, thereby increasing risks of respiratory failure and acute respiratory distress syndrome (ARDS). Simultaneous immune response to dual viral pathogens might compromise host defenses, elevating susceptibility to secondary bacterial infections (*e.g.*, *Streptococcus pneumoniae*). Coinfection with influenza A virus enhances SARS-CoV-2 infectivity [4–7]. Current therapeutic strategies for coinfection recommend combination therapy incorporating anti-influenza agents (*e.g.*, oseltamivir) and anti-COVID-19 medications (*e.g.*, paxlovid) [1]. To date, no therapeutic agents specifically targeting the coinfection have received regulatory approval. More seriously, the overlapping epidemic seasons of the influenza virus and SARS-CoV-2 create an urgent need for novel therapeutic strategies to treat SARS-CoV-2 and influenza virus coinfection.

Pyrimidines, essential components of intracellular bioactive molecules, participate in the biosynthesis of DNA, RNA, polysaccharides, and phospholipids, playing a pivotal role in human metabolism [7]. Cellular pyrimidine nucleotide synthesis occurs *via* two distinct pathways: the salvage pathway and *de novo* synthesis. In quiescent or fully differentiated cells, *de novo* synthesis ex-

* Corresponding authors.
E-mail addresses: leizhao-hit@hotmail.com (L. Zhao), dawei1105@foxmail.com (Y. Gao), zhongwu@bmi.ac.cn (W. Zhong).
[1] These authors contributed equally to this work.

https://doi.org/10.1016/j.cclet.2025.111751
1001-8417/© 2026 Published by Elsevier B.V. on behalf of Chinese Chemical Society and Institute of Materia Medica, Chinese Academy of Medical Sciences.

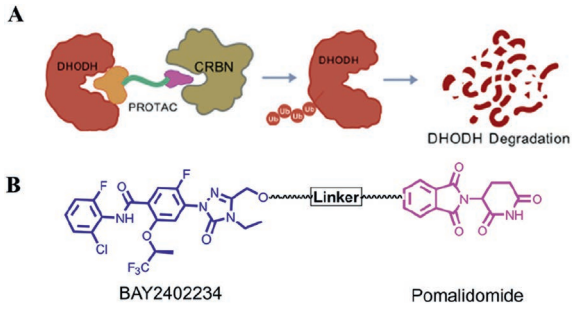


Fig. 1. (A) Schematic representation of DHODH PROTAC. (B) Design of DHODH PROTACs based upon BAY2402234 and pomalidomide.

hibits low activity, with pyrimidine demands predominantly met by the salvage pathway. However, proliferative cells (*e.g.*, tumor cells) and viruses necessitate *de novo* pyrimidine biosynthesis to sustain their heightened requirements for nucleic acid precursors and cellular components [8–11]. Human dihydroorotate dehydrogenase (DHODH) is the rate-limiting enzyme in the fourth step of *de novo* pyrimidine synthesis, catalyzes the oxidation of dihydroorotate to orotate. In virus-infected cells, rapid viral replication imposes an extraordinary demand for nucleosides to sustain high metabolic turnover, rendering *de novo* biosynthesis more critical than the salvage pathway for viral propagation. As the key enzyme in this pathway, DHODH has emerged as a compelling broad-spectrum host antiviral target, with its inhibitors displaying antiviral potential [12–19]. Although these inhibitors exhibit substantial antiviral activity, but still face limitations.

In our previous studies [20], we found that the DHODH inhibitor BAY2402234 exhibits anti-influenza virus and SARS-CoV-2 activity with considerably low half maximal effective concentration (EC_{50}) values. But, the 90% maximal effective concentration (EC_{90}) and 95% maximal effective concentration (EC_{95}) values exhibited a 10-fold or more increase compared to the EC_{50}. This indicates that while DHODH inhibitor possesses inhibitory activity against viruses, it fails to achieve complete viral clearance, thereby compromising its clinical efficacy. Furthermore, the inhibitors block the catalytic function of DHODH by binding to its active site, but the protein itself still exists, which may retain the non-enzymatic functions or restore activity through other pathways. In addition, long-term use of inhibitors may lead to target mutation or the activation of compensatory pathways, which may induce drug resistance [21,22]. Hence, a novel strategy targeting DHODH is required to remedy the limitations of inhibitors and thereby achieve complete viral eradication.

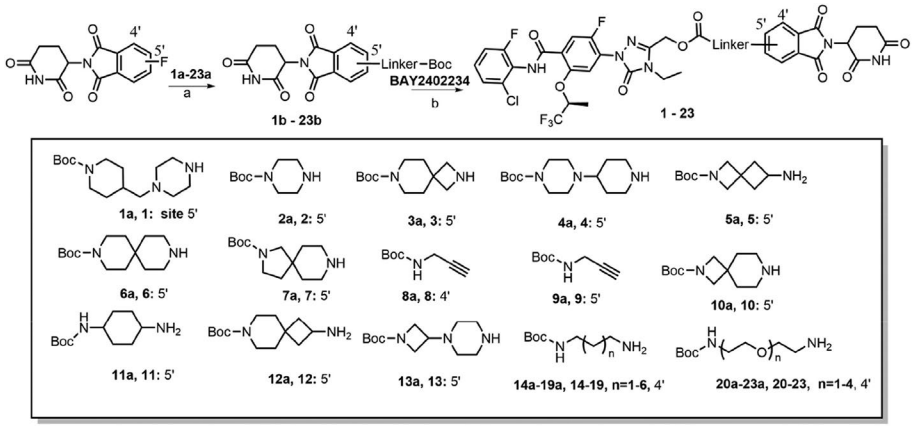
Proteolysis-targeting chimeras (PROTACs) have emerged as a robust strategy for selectively degrading disease-associated proteins, garnering significant momentum in drug discovery [23–28]. PROTAC degraders comprise two interconnected recruitment modules: one binds to the protein of interest (POI), while the other engages an E3 ubiquitin ligase. These bifunctional compounds facilitate E3 ligase recruitment, enabling POI ubiquitination and subsequent degradation *via* the ubiquitin-proteasome system (UPS) (Fig. 1A). A hallmark of PROTACs lies in their catalytic capability to eliminate entire POI, thereby potently inhibiting both catalytic and non-enzymatic functions [29–32]. BAY2402234 is a novel and potent DHODH inhibitor with antiviral activity [13,33,34]. Preclinical studies revealed BAY2402234′s superior efficacy and pharmacokinetic profile compared to other DHODH inhibitors, prompting its selection as the DHODH ligand in this study. We systematically conjugated BAY2402234 to cereblon (CRBN) E3 ligase ligands using diverse linker systems to construct DHODH PROTACs, enabling structure-degradation relationship analysis (Fig. 1B). The synthesis of PROTACs **1**–**23** followed the routes outlined in Scheme 1. Boc-protected linkers underwent nucleophilic substitution with pomalidomide derivatives to yield intermediate conjugates. Then, Boc-deprotection and coupling with BAY2402234 (synthesized in-house) afforded the final compounds **1**–**23**.

Studies have demonstrated that the introduction of conformationally rigid linkers in PROTAC degraders can improve the degradation efficacy, selectivity, and pharmacokinetic properties [35,36]. Therefore, we first employed linkers with varying rigidities, including monocyclic, spirocyclic, and bicyclic structures possessing comparable spatial spans, to conjugate BAY2402234 to the 5′-position of pomalidomide, thereby designed and synthesized a series of DHODH PROTAC degraders. Subsequently, we use the HEK293T cell line to evaluate the degradation efficiency of these PROTACs. Following 24 h treatment with 1 μmol/L PROTACs in HEK293T cells, the DHODH protein level was determined *via* Western blot (WB) analysis (Figs. 2A and B), the degradation efficiency was summarized in Table S1 (Supporting information). The results revealed that this compound series (**1**–**13**) exhibited limited DHODH degradation activity. This diminished efficacy may be attributed to the rigid linker architecture, which potentially reduces molecular flexibility and restricts critical spatial parameters (*e.g.*, distance and orientation between interacting moieties), thereby impeding optimal ternary complex formation. Furthermore, such structural rigidity might compromise cellular permeability of the molecules.

The flexibility of the linkers enables PROTAC molecules to achieve greater spatial adjustability when simultaneously binding to both the target protein and E3 ligase, thereby optimizing molecular activity and reactivity. This characteristic facilitates enhanced ubiquitination efficiency and degradation efficacy of the target protein [36,37]. **8** and **9** in previous series share an identical linker but differ in their attachment site to the CRBN ligand. **8** attached at the 4′-position of pomalidomide, exhibits superior degradation activity compared to **9** attached at the 5′-position. This suggests that linkage at the 4′-position of the CRBN ligand may be more favorable for ternary complex formation. Furthermore, literature reports [38] indicate that derivatives linked at the 4′-position of pomalidomide demonstrate greater structural stability and enhanced degradation potency compared to those linked at the 5′-position. Subsequently, we selected flexible alkyl chains and PEG chains with different lengths, and switched the connection point from the 5′-position of pomalidomide to the 4′-position to further prepare PROTACs **14**–**23**. These PROTACs demonstrated superior DHODH degradation activities compared to previous series (Figs. 2A and B). The degradation efficiency was summarized in Table S2 (Supporting information). These results indicate that PROTACs have flexible linkers of appropriate length, and the flexible molecular conformation may perform better in recruiting DHODH and CRBN to form a ternary complex, thus making the better degradation activity.

In the preliminary anti-SARS-CoV-2 and degradation efficiency screening, all of these PROTACs demonstrated anti-SARS-CoV-2 activities at the same level (Table S3 in Supporting information). Among them, **17** and **19** consistently maintained stable and significant degradation activities and were identified as the most effective molecules (Figs. S1–S3 in Supporting information). The results showed that **17** and **19** effectively degraded DHODH at 0.3 and 1.1 μmol/L, respectively (Fig. 3A) and both showed “hook effect”. Similarly, **17** and **19** could also effectively degrade the DHODH in MDCK cells (Fig. S4 in Supporting information). We further investigated the mechanism of **17** and **19** induced DHODH degradation. Pretreatment with the proteasome inhibitor MG132 and CRBN ligand pomalidomide rescued DHODH degradation mediated by **17** and **19**, demonstrated that **17** and **19** induced DHODH degradation through the proteasome and CRBN-dependent mechanisms (Fig. 3B and Fig. S5 in Supporting information).

Since PROTACs **17** and **19** exhibit promising degradation activities, we further validated their broad-spectrum antiviral ac-



Scheme 1. Synthesis of compounds **1**–**23**. Reagents and conditions: (a) 2-(2,6-dioxopiperidin-3-yl)-4-fluoroisoindoline-1,3–dione, DIPEA, DMF, 85 °C, 4 h, 71 %–88 %; (b) (1) trifluoroacetic acid (TFA), dichloromethane (CH_2Cl_2), room temperature (r.t.), 4 h; (2) BAY2402234, triphosgene, DIPEA, DMF, N_2, 0 °C–r.t., 3 h, 35 %–46 % (two steps).

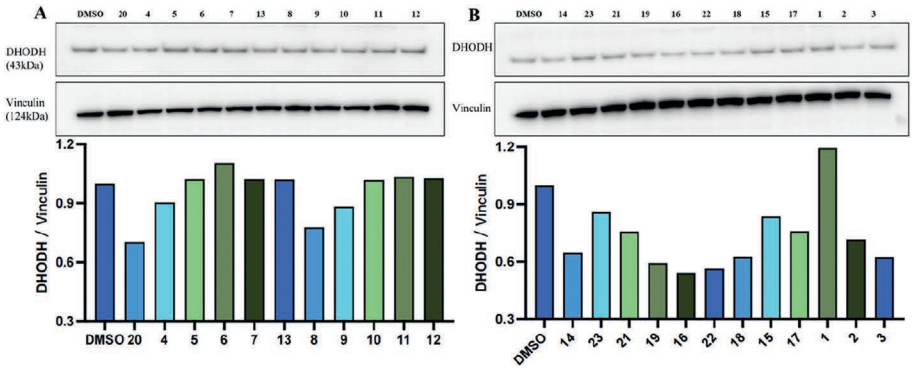


Fig. 2. (A, B) The DHODH protein level was determined by WB after treatment with compounds at 1 μmol/L in HEK293T cells for 24 h.

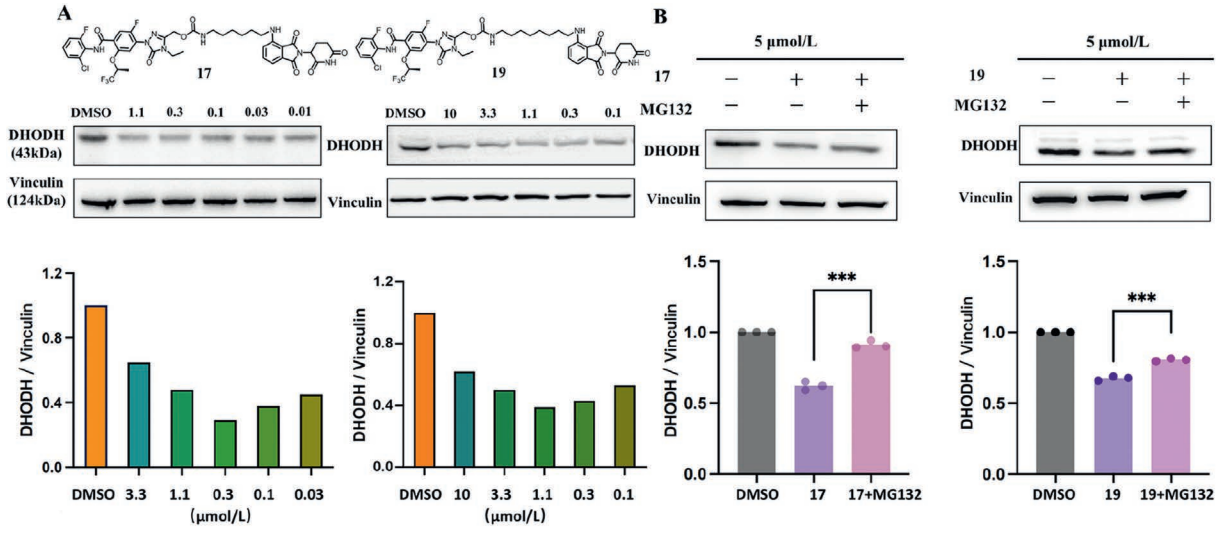


Fig. 3. (A) WB analysis of DHODH in HEK293T cell lines treated with PROTACs **17** and **19** at different concentration for 48 h. (B) Mechanism investigation of **17** and **19**, the cells were pretreated with 5 μmol/L MG132 for 2 h, followed by 5 μmol/L **17** and **19** treatment for 48 h. Data are presented as mean ± standard deviation (SD) ($n = 3$). $^{***}P < 0.001$.

tivity against influenza A and B viruses in the MDCK cell line. The results showed that **17** and **19** exhibited higher EC_{50} values against B/Russia/69 (B/Russia), A/Hong Kong/8/68 (HK68) and A/California/07/2009 (CA07) strain than BAY2402234 (Fig. 4A), but their 70 % maximal effective concentration (EC_{70}), EC_{90} and EC_{95} values were very close to the EC_{50} level. Notably, **17** and **19** demonstrated lower EC_{90} and EC_{95} values compared to BAY2402234, demonstrating superior viral clearance capacity against influenza virus than BAY2402234 (Table 1). Meanwhile, the PROTACs **17** and **19** did not exhibit cytotoxicity at the concentration of 50 μmol/L (half maximal cytotoxic concentration (CC_{50}) > 50 μmol/L) in MDCK cells. Furthermore, we evaluated their anti-

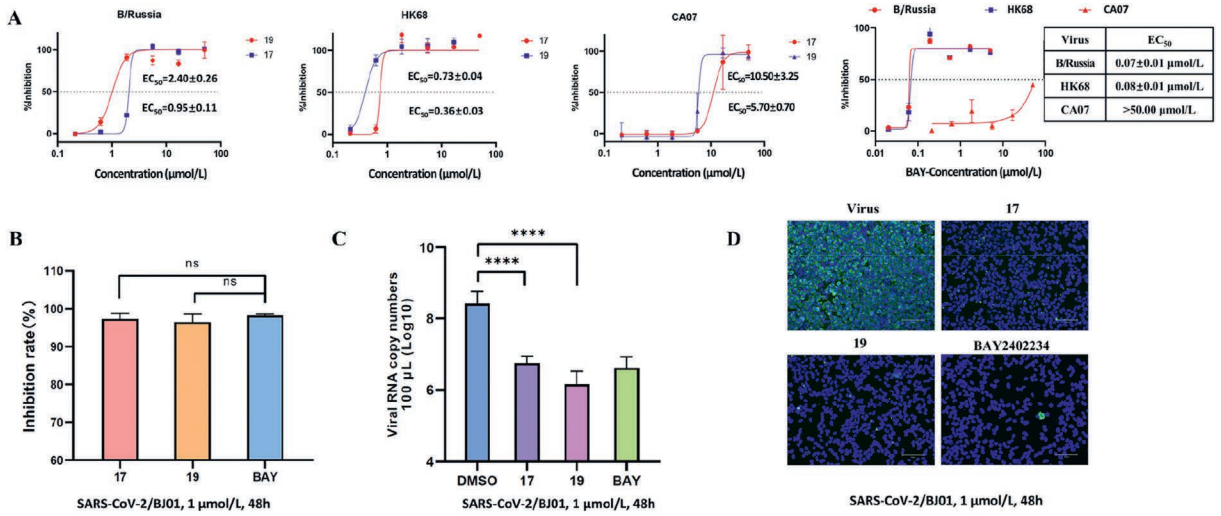


Fig. 4. Compounds **17** and **19** displayed potent broad-spectrum anti-influenza virus and anti-SARS-CoV-2 activity. (A) EC_{50} of **17**, **19** and BAY2402234 against B/Russia/69, A/Hong Kong/8/68 and A/California/07/2009. (B) Inhibition rate of **17**, **19** and BAY2402234 against SARS-CoV-2/BJ01. (C) **17**, **19** and BAY2402234 reducing viral RNA copies and (D) inhibiting viral protein expression (SARS-CoV-2/BJ01 strain in 293T-ACE2 cells, 1 μmol/L, 48 h. Data are expressed as mean ± SEM ($n = 3$). $^{****}P < 0.0001$. Cells were fixed and permeabilized for staining with an anti-viral N protein antibody, followed by staining with Alexa 488-labeled secondary antibody. Green represents the virus in infected cells. Nuclei were stained by 4′,6-diamidino-2-phenylindole (DAPI), and the merged of N protein and nuclei were shown. Scale bar: 100 μm. ns, no significance.

Table 1
EC_{70}, EC_{90} and EC_{95} values of **17**, **19** and BAY2402234 against different influenza viral strains.[a]

Compound	B/Russia (μmol/L)			HK68 (μmol/L)			CA07 (μmol/L)		
	EC_{70}	EC_{90}	EC_{95}	EC_{70}	EC_{90}	EC_{95}	EC_{70}	EC_{90}	EC_{95}
17	2.79 ± 0.46	3.37 ± 0.74	3.64 ± 0.86	0.76 ± 0.05	0.79 ± 0.05	0.80 ± 0.06	11.90 ± 4.25	15.16 ± 6.93	19.48 ± 1.96
19	1.15 ± 0.17	1.33 ± 0.27	1.57 ± 0.39	0.46 ± 0.05	0.64 ± 0.08	0.71 ± 0.09	5.84 ± 1.06	6.10 ± 4.21	6.39 ± 2.27
BAY2402234	0.08 ± 0.01	>5.00	>5.00	0.12 ± 0.04	>5.00	>5.00	>50.00	>50.00	>50.00

[a] The antiviral assay was conducted in the MDCK cell line.

Table 2
In vivo PK parameters of **17** and **19** following i.v. administration to rats at 1 mg/kg ($n = 3$).

Compound	C_0 (ng/mL)[a]	$t_{1/2}$ (h)[b]	Cl (mL min^{-1} kg^{-1})[c]	*Vss* (L/kg)[d]	AUC_{last} (h ng mL^{-1})[e]
17	361 ± 89	3.08 ± 0.24	117 ± 10	9.5 ± 2.4	138 ± 12
19	339 ± 31	3.20 ± 0.16	117 ± 9	10.6 ± 1.3	139 ± 11

[a] Initial *in vivo* plasma concentration.
[b] *In vivo* half-life.
[c] *In vivo* clearance value.
[d] *In vivo* volume of distribution.
[e] *In vivo* exposure measured over 24 h time period. Formulation = 5 % DMSO + 10 % solutol + 85 % saline.

SARS-CoV-2 efficacy through indirect immunofluorescence assays and real-time quantitative PCR experiments. The results demonstrated that in SARS-CoV-2/BJ01 infected 293T-ACE2 cells, **17** and **19** exhibited anti-SARS-CoV-2 activities comparable to BAY2402234 at the concentration of 1 μmol/L, significantly reducing viral RNA copies and inhibiting viral protein expression (Figs. 4B–D). Collectively, these findings suggest the potential of **17** and **19** for treating influenza virus and SARS-CoV-2 infection.

It is common knowledge that PROTAC molecules belong to "beyond Rule of 5″ (bRo5) chemical space. Their large and flexible structure is responsible for drug metabolism and pharmacokinetics limitations [39]. We further evaluated the *in vivo* pharmacokinetics (PK) properties of **17** and **19** through single-dose intravenous administration (1 mg/kg, i.v.) in Sprague Dawley rats. Animal research has been approved by the Animal Care Committee of the Beijing Institute of Biotechnology. All operations were following the Animal Care and Use Committee Guidelines of China. As shown in Table 2, both **17** and **19** showed a moderate $t_{1/2}$ (3.08 and 3.20 h, respectively). However, the clearance rate indicates that the metabolic profiles of **17** and **19** in rats are less favorable. Potentially, the complex spatial structure of PROTACs precisely provides the binding sites required by the enzymatic active center, which facilitates their binding and catalyzes the metabolic process [39].

In summary, we reported the discovery of novel PROTAC degraders with broad-spectrum anti-influenza virus and anti-SARS-CoV-2 activities by degrading DHODH. The structure-degradation relationship analysis revealed that PROTACs connected by flexible linkers with appropriate lengths demonstrated enhanced degradation efficacy compared to those with rigid linkers, due to their superior conformational adaptability. Mechanistic studies revealed that **17** and **19** selectively induced DHODH degradation in a proteasome- and CRBN-dependent manner. Significantly, **17** and **19** exhibit enhanced capacity for complete viral eradication against influenza virus compared to BAY2402234 and comparable anti-SARS-CoV-2 activities to BAY2402234, demonstrating therapeutic potential for influenza virus and SARS-CoV-2 infection. Moreover, **17** and **19** achieved moderate $t_{1/2}$ in rats. Collectively, PROTACs **17** and **19** serve as viable initial lead compounds for further optimization, of-

fering a new strategy for treating SARS-CoV-2 and influenza virus coinfection.

Declaration of competing interest

The authors declare that they have no known competing financial interests or personal relationships that could have appeared to influence the work reported in this paper.

CRediT authorship contribution statement

Hongliang Wang: Writing – review & editing, Writing – original draft, Methodology, Investigation, Formal analysis. **Yuanguo Li:** Writing – original draft, Formal analysis, Data curation. **Linjie Yan:** Writing – review & editing, Writing – original draft, Investigation. **Liyuan Ge:** Writing – original draft, Visualization, Data curation. **Wenhao Wang:** Visualization, Methodology, Data curation. **Lei Zhao:** Writing – review & editing, Visualization, Software, Investigation, Formal analysis, Conceptualization. **Yuwei Gao:** Writing – review & editing, Visualization, Investigation, Conceptualization. **Wu Zhong:** Writing – review & editing, Supervision, Resources, Project administration, Methodology, Funding acquisition, Conceptualization.

Acknowledgments

This work was supported by the Key project of National Natural Science Foundation of China (No. 82341102). We thank Beijing Sunho Pharmaceutical Co., Ltd. for their technical support and expertise in protein degradation analysis.

Supplementary materials

Supplementary material associated with this article can be found, in the online version, at doi:10.1016/j.cclet.2025.111751.

References

[1] S. Liu, W. Li, S. Jiang, J. Med. Virol. 94 (2022) 4056–4057.
[2] M. Golpour, Jalali H, R. Alizadeh-Navaei, et al., BMC Infect. Dis. 25 (2025) 145.
[3] K.L. Mai, W.Q. Pan, S.L. Zheng, et al., Adv. Biotechnol. 3 (2025) 5.
[4] M.C. Swets, C.D. Russell, E.M. Harrison, et al., Lancet 399 (2022) 1463–1464.
[5] G.W. Pratt, C.L. Wong, L.V. Rao, APMIS 133 (2025) e70010.
[6] H.C. Maltezou, A. Papanikolopoulou, S. Vassiliu, et al., Viruses 15 (2023) 865.
[7] L. Bai, Y.L. Zhao, J.Z. Dong, et al., Cell Res. 31 (2021) 395–403.
[8] Y. Zhou, L. Tao, X. Zhou, et al., Cancer Metab. 9 (2021) 22.
[9] J. Fang, T. Uchiumi, M. Yagi, et al., Biosci. Rep. 33 (2013) e00021.
[10] V.K. Vyas, M. Ghate, Mini Rev. Med. Chem. 11 (2011) 1039–1055.
[11] F. Zeng, S. Li, G. Yang, et al., Acta Pharm. Sin. B 11 (2021) 795–809.
[12] R. Xiong, L.K. Zhang, S.L. Li, et al., Protein Cell 13 (2022) 778.
[13] Y.C. Zheng, S.L. Li, K. Song, et al., Viruses 14 (2022) 928.
[14] M. Qing, G. Zou, Q.Y. Wang, et al., Antimicrob. Agents Chemother. 54 (2010) 3686–3695.
[15] P.I. Andersen, K. Krpina, A. Ianevski, et al., Viruses 11 (2019) 964.
[16] D.Morales Vasquez, J.G. Park, G. Ávila-Pérez, et al., Viruses 12 (2020) 1041.
[17] P. Luthra, J. Naidoo, C.A. Pietzsch, et al., Antiviral Res. 158 (2018) 288–302.
[18] H. Fu, Z. Zhang, Y. Dai, et al., Am. J. Transl. Res. 12 (2020) 8247–8255.
[19] J. Luban, R.A. Sattler, E. Mühlberger, et al., Virus Res. 292 (2021) 198246.
[20] W. Zhong, X.B. Zhou, R.Y. Cao, et al., Patent, US2022193039A1, 2020.
[21] R.A. Ward, S. Fawell, N. Floc'h, et al., Chem. Rev. 121 (2021) 3297–3351.
[22] Y. Yang, S. Li, Y. Wang, et al., Signal Transduct. Target Ther. 7 (2022) 329.
[23] M. Békés, D.R. Langley, C.M. Crews, Nat. Rev. Drug Discov. 21 (2022) 181–200.
[24] M. Konstantinidou, J.Y. Li, B.D. Zhang, et al., Expert. Opin Drug Discov. 14 (2019) 1255–1268.
[25] K. Li, C.M. Crews, Chem. Soc. Rev. 51 (2022) 5214–5236.
[26] L. Zhao, J. Zhao, K.H. Zhong, et al., Signal Transduct. Target. Ther. 7 (2022) 113.
[27] K.L. Li, G.Q. Dong, S.C. Wu, et al., Chin. Chem. Lett. 36 (2025) 110280.
[28] Y.Y. Yang, H.R. Xie, X.B. Yu, et al., Chin. Chem. Lett. 35 (2024) 109570.
[29] S.B. Alabi, C.M. Crews, J. Biol. Chem. 296 (2021) 100647.
[30] H.Y. Zhao, M.H. Xin, S.Q. Zhang, Drug Dev. Res. 84 (2023) 337–394.
[31] Z.Y. Kang, S. Li, Y. Li, et al., Chin. Chem. Lett. 36 (2025) 110447.
[32] X.Y. Shao, S.J. Xu, X.F. Wan, et al., Chin. Chem. Lett. 34 (2023) 108349.
[33] S. Christian, C. Merz, L. Evans, et al., Leukemia 33 (2019) 2403–2415.
[34] K.M. Stegmann, A. Dickmanns, N. Heinen, et al., iScience 25 (2022) 104293.
[35] T.A. Bemis, J. La Clair, M.D. Burkart, J. Med. Chem. 64 (2021) 8042–8052.
[36] K. Cyrus, M. Wehenkel, E.Y. Choi, et al., Mol. BioSyst. 7 (2011) 359–364.
[37] V. Poongavanam, Y. Atilaw, S. Siegel, et al., J. Med. Chem. 65 (2022) 13029–13040.
[38] A. Bricelj, Y.L. Dora Ng, D. Ferber, et al., ACS Med. Chem. Lett. 12 (2021) 1733–1738.
[39] V. Poongavanam, B.C. Doak, J. Kihlberg, Curr. Opin. Chem. Biol. 44 (2018) 23–29.